Morphological and Transistor Studies of Organic Molecular Semiconductors with Anisotropic Electrical Characteristics

X. Linda Chen, Andrew J. Lovinger,* Zhenan Bao,* and Joyce Sapjeta

Bell Laboratories, Lucent Technologies, 600 Mountain Avenue, Murray Hill, New Jersey 07974

Received October 26, 2000. Revised Manuscript Received February 6, 2001

Oriented thin films of organic semiconducting small molecules were prepared by crystallization on rubbed alignment layers. Polarized absorption spectra showed that the long axis of the conjugated backbones was highly oriented along the rubbing direction and parallel to the substrates. Transmission electron microscopy and diffraction confirmed that the molecules and in many cases the resulting crystals are aligned. Using the above aligned films as semiconducting layers, we fabricated field-effect transistors having anisotropic mobilities with ratios greater than 15. Several common organic semiconductors have been investigated, and the results indicate that this growth method is generally successful for achieving macroscopic alignment of these semiconducting molecules (and frequently their crystals, as well).

Introduction

Recently, great progress has been made in the field of organic field-effect transistors.[1−8] Both n-type [8−11] and p-type [12−20] organic semiconductors with mobilities greater than 0.01 $cm^2/(V\ s)$ and on/off ratios above 10^3 have been realized. Integrated circuits, such as complementary inverters, ring oscillators, and shift registers, have been demonstrated.[5,21−23] This opens up possibilities for use of these devices in practical applications, such as low-cost large area flexible displays and low-end data storage.

In organic transistor devices, the electrical behavior is governed by the electronic states of the semiconducting molecules and the morphology of their thin films.[12] It is generally believed that charge transport in organic materials is realized by $\pi-\pi$ interactions between molecules through the hopping mechanism. This is in sharp contrast to the conventional inorganic semiconductors that rely on bandlike transport. During the hopping process, charges propagate preferentially along the stacking axis of molecules through their overlapping π-orbitals. It has been widely shown that the structural organization of molecules plays an important role in this process.[1] The charge carrier mobilities are highly dependent on the molecular orientation and crystal grain size, which in turn depend on the chemical structures of the constituent molecules and the deposition parameters.[15,24]

Investigations of electronic and optical devices based on oriented organic semiconductors have been widely pursued because they offer novel properties, such as polarized light emission from light-emitting diodes, [25−28]

(1) Bao, Z. *Adv. Mater.* **2000**, *12*, 227.
(2) Katz, H. E.; Bao, Z. *J. Phys. Chem. B* **2000**, *104*, 671−678.
(3) Brown, A. R.; Jarrett, C. P.; deLeeuw, D. M.; Matters, M. *Synth. Met.* **1997**, *88*, 37−55.
(4) Horowitz, G. *J. Mater. Chem.* **1999**, *9*, 2021−2026.
(5) Klauk, H.; Jackson, T. N. *Solid State Technol.* **2000**, *43*, 63.
(6) Katz, H. E.; Dodabalapur, A.; Bao, Z. In *Handbook of Oligo- and Polythiophenes*; Fichou, D., Ed.; Wiley-VCH: Weinheim, 1998.
(7) Lovinger, A. J.; Rothberg, L. J. *J. Mater. Res.* **1996**, *11*, 1581−1592.
(8) Bao, Z.; Lovinger, A. J.; Brown, J. *J. Am. Chem. Soc.* **1998**, *120*, 207−208.
(9) Katz, H. E.; Lovinger, A. J.; Johnson, J.; Kloc, C.; Siegrist, T.; Li, W.; Lin, Y. Y.; Dodabalapur, A. *Nature* **2000**, *404*, 478−481.
(10) Laquindanum, J. G.; Katz, H. E.; Dodabalapur, A.; Lovinger, A. J. *J. Am. Chem. Soc.* **1996**, *118*, 11331−11332.
(11) Haddon, R. C.; Perel, A. S.; Morris, R. C.; Palstra, T. T. M.; Hebard, A. F.; Fleming, R. M. *Appl. Phys. Lett.* **1995**, *67*, 121.
(12) Torsi, L.; Dodabalapur, A.; Rothberg, L. J.; Fung, A. W. P.; Katz, H. E. *Science* **1996**, *272*, 1462−1464.
(13) Gundlach, D. J.; Lin, Y. Y.; Jackson, T. N.; Schlom, D. G. *Appl. Phys. Lett.* **1997**, *71*, 3853−3855.
(14) Bao, Z.; Lovinger, A. J.; Dodabalapur, A. *Appl. Phys. Lett.* **1996**, *69*, 3066−3068.
(15) Lin, Y. Y.; Gundlach, D. J.; Nelson, S. F.; Jackson, T. N. *IEEE Electron Device Lett.* **1997**, *18*, 606−608.
(16) Bao, Z.; Dodabalapur, A.; Lovinger, A. J. *Appl. Phys. Lett.* **1996**, *69*, 4108.
(17) Dimitrakopoulos, C. D.; Afzali-Aradakani, A.; Furman, B.; Kymissis, J.; Purushothaman, S. *Synth. Met.* **1997**, *89*, 193.
(18) Brown, A. R.; deLeeuw, D. M.; Havinga, E. E.; Pomp, A. *Synth. Met.* **1994**, *68*, 65.
(19) Sirringhaus, H.; Friend, R. H.; Li, X. C.; Moratti, S. C.; Holmes, A. B.; Feeder, N. *Appl. Phys. Lett.* **1997**, *71*, 3871.
(20) Garnier, F.; Yassar, A.; Hajlaoui, R.; Horowitz, G.; Deloffre, F.; Servet, B.; Ries, S.; Alnot, P. *J. Am. Chem. Soc.* **1993**, *115*, 8716−8721.
(21) Lin, Y. Y.; Dodabalapur, A.; Sarpeshkar, R.; Bao, Z.; Li, W.; Baldwin, K.; Raju, V. R.; Katz, H. E. *Appl. Phys. Lett.* **1999**, *74*, 2714−2716.
(22) Crone, B.; Dodabalapur, A.; Lin, Y. Y.; Filas, R. W.; Bao, Z.; LaDuca, A.; Sarpeshkar, R.; Katz, H. E.; Li, W. *Nature* **2000**, *403*, 521−523.
(23) Drury, C. J.; Mutsaers, C. M. J.; Hart, C. M.; Matters, M.; de Leeuw, D. M. *Appl. Phys. Lett.* **1998**, *73*, 108.
(24) Bao, Z.; Lovinger, A. J.; Dodabalapur, A. *Adv. Mater.* **1997**, *9*, 42−44.
(25) Era, M.; Tsutsui, T.; Saito, S. *Appl. Phys. Lett.* **1995**, *67*, 2436−2438.
(26) Grell, M.; Knoll, W.; Lupo, D.; Meisel, A.; Miteva, T.; Neher, D.; Nothofer, H. G.; Scherf, U.; Yasuda, A. *Adv. Mater.* **1999**, *11*, 671.
(27) Cimrova, V.; Remmers, M.; Neher, D.; Wegner, G. *Adv. Mater.* **1996**, *8*, 146-&.

10.1021/cm0008563 CCC: $20.00
Published on Web 03/22/2001

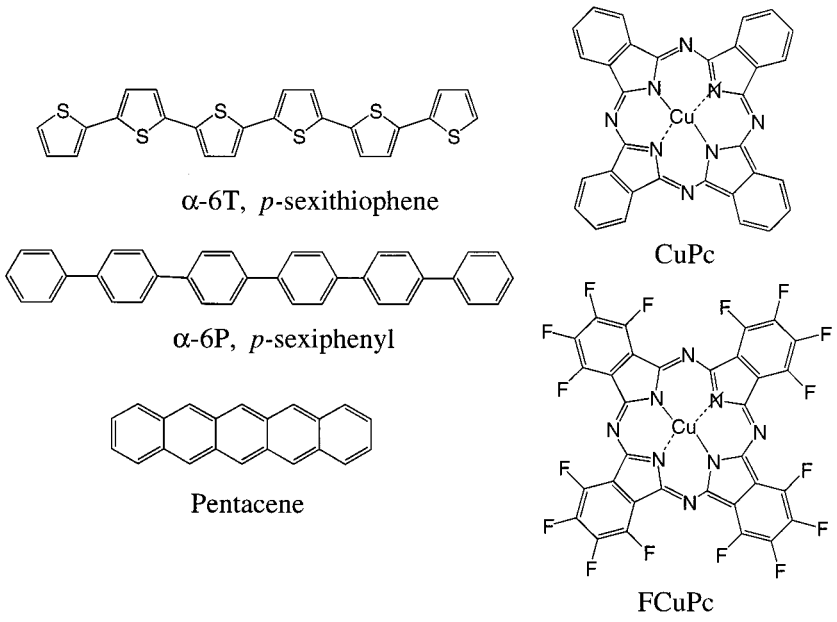

Figure 1. Chemical structures of the organic semiconducting molecules aligned by the rubbing technique.

or anisotropic charge transport in thin film transistors (TFTs).[29,30] Several methods have been used to obtain aligned films, such as mechanical stretching, [28,29] Langmuir−Blodgett (LB) deposition,[27,31] rubbing,[25] and liquid-crystalline self-organization. [26] Dyreklev et al. reported a TFT based on an oriented polythiophene derivative prepared by mechanical stretching.[29] Mobilities in the range of 10^{-5} cm^2/(V s) and an anisotropy ratio of about 4 were achieved.[29] Amundson et al. [32] used friction-transferred poly(tetrafluoroethylene) (PTFE) as an alignment layer to induce orientation in semiconducting polymers for TFT fabrication. However, thin films prepared by these approaches yielded poor device performance and nonuniform device characteristics.[29,32] Furthermore, previous efforts were mainly focused on the alignment techniques and the optical and electrical properties of the aligned films; [25−33] few have studied the morphology of the oriented films.

Here, we apply a method to control both the molecular and crystal orientation of organic semiconductors, producing films with strong anisotropy of the field-effect mobility. In some cases, enhanced mobilities can be obtained. This approach was also independently used by Fichou et al. to enhance the light absorption and charge transport of α-6T photovoltaic cells.[33] Electrical and morphological properties of these aligned films were studied in context. Improved mobilities with anisotropic ratios greater than 15 were achieved. The electrical characteristics were directly correlated to the morphology of their aligned films. The anisotropic mobility could be useful in isolating neighboring components so as to reduce cross-talk.

The molecules chosen for alignment studies (see Figure 1) include rodlike α-6T[20,34,12] and *p*-sexiphenyl (α-6P),[13] boardlike pentacene,[15] and disk-shaped copper phthalocyanine (CuPc)[14,24] and copper hexadecafluorophthalocyanine (FCuPc).[8] They all have been reported as promising candidates for TFT applications with mobilities well above 0.01 cm^2/(V s) and on/off ratios greater than 1000. α-6T, α-6P, pentacene, and CuPc are p-type semiconductors, whereas FCuPc is n-type.

Experimental Section

α-6T was synthesized according to literature procedures[35] and purified by vacuum sublimation. α-6P (TCI America Chemical Co.), pentacene (Aldrich Chemical Co.), CuPc (Aldrich Chemical Co.), and FCuPc (Aldrich Chemical Co.) were purchased commercially and purified by vacuum sublimation. An *n*-doped Si wafer with a thermally grown silicon dioxide layer (300 nm thick, 11 nF/cm^2 capacitance) was used as the substrate. A thin organic semiconductor layer (5 nm) was first deposited at a rate of 0.1−0.2 nm/s under a vacuum of 2.0×10^{-6} Torr. A Teflon bar was then gently slid over this thin layer a dozen times. An additional layer of the same organic compound was subsequently evaporated to a final thickness of 50 nm. In another approach, a soft-hair brush purchased from VWR Scientific Co. was used instead of the Teflon bar. All substrates were held at room temperature during deposition. Gold electrodes were thermally evaporated onto the semiconducting layer through a regular square-grid array shadow mask to form source and drain contacts and complete the devices. The channels of the transistors were aligned parallel or perpendicular to the rubbing direction. The I-V characteristics of the TFTs were obtained by using a HP 4155A semiconductor parameter analyzer.

Optical absorption spectra were recorded with an HP-8453 spectrometer. Atomic force micrographs (AFM) were obtained from the films using a Digital Instruments Nanoscope III in the tapping mode. Etched Si cantilevers of 125 mm in length and resonant frequencies between 300 and 350 kHz were used to obtain height and phase contrast images.

For electron microscopy and diffraction, films were first deposited onto freshly cleaved mica substrates. They were

(28) Dyreklev, P.; Berggren, M.; Inganas, O.; Andersson, M. R.; Wennerstrom, O.; Hjertberg, T. *Adv. Mater.* **1995**, *7*, 43−45.
(29) Dyreklev, P.; Gustafsson, G.; Inganas, O.; Stubb, H. *Synth. Met.* **1993**, *57*, 4093−4098.
(30) Sirringhaus, H.; Wilson, R. J., Friend, R. H.; Inbasekaran, M.; Wu, W.; Woo, E. P.; Grell, M.; Bradley, D. D. C. *Appl. Phys. Lett.* **2000**, *77*, 406−408.
(31) Xu, G.; Bao, Z.; Groves, J. T. *Langumir* **2000**, *16*, 1834−1841.
(32) Amundson, K.; Lovinger, A. J.; Sapjeta, J.; Bao, Z. Submitted to *Thin Solid Films*.
(33) Videlot, C.; Fichou, D. *Synth. Met.* **1999**, *102*, 885−888.
(34) Horowitz, G. *Solid State Commun* **1989**, *72*, 381.
(35) Katz, H. E.; Torsi, L.; Dodabalapur, A. *Chem. Mater.* **1995**, *7*, 2235−2237.

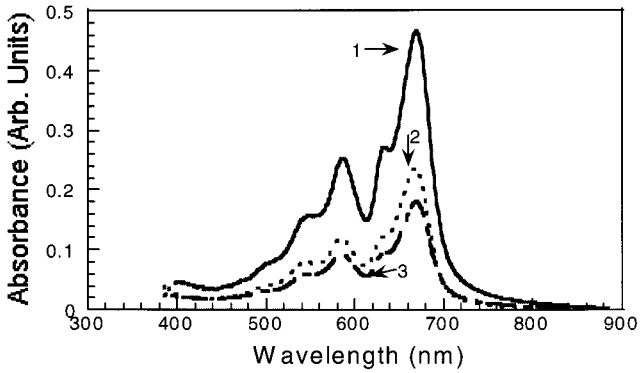

Figure 2. Polarized absorption spectra of a rubbed film of pentacene. Curves 1 and 2 are obtained with polarized light parallel and perpendicular to the rubbing directions, respectively. Also plotted in this figure is the absorption spectrum of a nonrubbed control sample of pentacene (curve 3).

shadowed with Pt/C and carbon-coated in a vacuum evaporator, floated off their mica substrates in water, caught onto electron-microscope grids, and finally examined at 100 kV in a JEOL transmission electron microscope.

Results and Discussion

I. Optical and Surface Properties. Thin films of the aligned small molecules were examined by polarized UV−vis spectroscopy and atomic force microscopy. Under visual observations, the rubbed films appear transparent and uniform. However, in the polarizing microscope streaked birefringent features were seen. As the samples were rotated, complete extinction was obtained when the rubbing direction became parallel to the polarizers.

Absorption measurements performed on these aligned films (ca. 50 nm thick) indicate that the transition dipoles (corresponding to the molecular axes) are aligned parallel to the rubbing direction. Figure 2 shows the UV−vis absorption spectra of an oriented pentacene film taken at normal incident angle with the polarized light source. For comparison, the UV−vis absorption spectrum of a nonrubbed pentacene sample is also plotted in Figure 2. The absorption intensity of the reference sample is lower than that of aligned pentacene film with the same thickness, indicating that the molecular axis becomes parallel and more inclined toward the substrate in the aligned film. Both types of film exhibit strong absorption bands at 500−700 nm with peak maxima at 585 and 669 nm. A moderate dichroic ratio of about 3 was obtained, with the higher intensity arising from the film with polarization direction parallel to the rubbing direction. This confirms that the molecular axis is aligned parallel to the rubbing direction. Absorption peak maxima and dichroic ratios of all aligned films are summarized in Table 1. We note from the results that the anisotropy ratio depends on the molecular shape. The films prepared from rodlike molecules such as α-6T and α-6P show the highest anisotropy (about 5). This ratio is reduced to 3 for boardlike pentacene and to only 1.5−2 for disklike CuPc and FCuPc.

Atomic force microscopy (AFM) provides more information on the rubbed prelayer. Figure 3 shows the AFM images of height (Figure 3a,c) and phase (Figure 3b,d) profiles for rubbed thin films (5 nm) of pentacene (Figure 3a,b) and FCuPc (Figure 3c,d). These films,

Table 1. Absorption λ_{max} and Dichroic Ratios for Various Rubbed Organic Small Molecules Measured at the Maximum Intensities of Absorption[a]

molecules	λ_{max} (nm, absorption)	polarization ratio
α-6T	380	5.0
α−6P	310	5.2
pentacene	585, 669	3.1
CuPc	622, 696	2.0
FCuPc	655, 792	1.5

[a] For molecules with more than one absorption peak, the intensity at the longest wavelength is used.

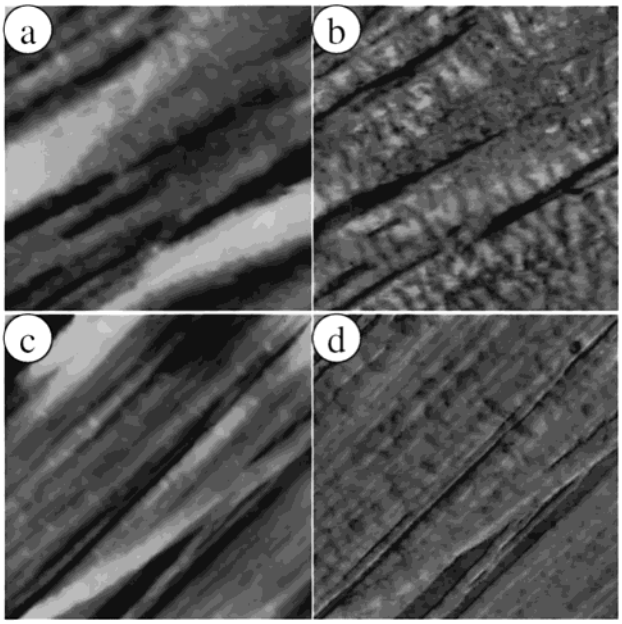

Figure 3. 0.5 μm × 0.5 μm AFM images of rubbed oriented 50 nm films of pentacene (a and b) and FCuPc (c and d) on Si wafers. (a) and (c) are height images with $Z = 20$ nm; (b) and (d) are phase-contrast images with $Z = 20$ nm and $Z = 10$ nm, respectively.

which are used as the alignment layers for subsequent deposition, consist of visible streaks 50−100 nm in width and at least 10 μm in length, with a root-mean-square roughness of 1.9 and 2.5 nm for pentacene and FCuPc, respectively. Parts of the film are seen to be overlying on top of other parts, probably as a result of repeated rubbing. Phase contrast images of these rubbed films show more clearly the resulting displacement of the film in some areas and the bare silicon surface thus exposed. The rubbed films have the appearance of long filaments of material, similar to the appearance of friction-transferred PTFE.[36] But our rubbing conditions used here are very different from the friction transfer of PTFE. In our case, the substrates were not heated and the Teflon bar was only very gently rubbed on the organic thin films. On the contrary, the substrate for the friction transfer method is usually heated to above 200 °C and pressure is applied to deposit a highly aligned PTFE layer.[37] While such PTFE films typically consist of completely featureless longitudinal filaments (see, e.g., Figure 1 of ref 39), small features are readily apparent on the rubbed surfaces of both the pentacene

(36) Chen, X. L.; Bao, Z.; Sapjeta, B. J.; Lovinger, A. J.; Crone, B. *Adv. Mater.* **2000**, *12*, 344.
(37) Wittmann, J. C.; Smith, P. *Nature* **1991**, *352*, 414−417.
(38) Horowitz, G.; Bachet, B.; Yassar, A.; Lang, P.; Demanze, F.; Fave, J. L.; Garnier, F. *Chem. Mater.* **1995**, *7*, 1337−1341.

and FCuPc films (Figure 3b,d), indicating that in our case these aligned fibers are not residual PTFE. The features observed in the AFM images are similar in appearance to the corresponding TEM images of the pentacene and FCuPc films (see Figures 7b and 9b). These observations suggest that our gentle room-temperature rubbing approach is a clean method for preparing the templating prelayer and does not introduce an intermediate layer of PTFE.

II. Transistor Characteristics. Using these aligned films as semiconducting layers, we have fabricated field-effect transistors on n-doped Si substrates with a thermally grown silicon dioxide layer. A rectangular square shadow mask is used for evaporation of gold drain and source electrodes. The current−voltage characteristics recorded for the devices based on α-6T, α-6P, pentacene, and CuPc exhibited typical p-channel transistor behavior in the accumulation mode, whereas FCuPc behaves as a typical n-channel semiconductor. The TFT characteristics for CuPc are shown in Figure 4, where the drain current is plotted as a function of drain-source voltage for several gate voltages. The field-effect mobilities were calculated in the saturation region using eq 1

$$I_{ds} = (W/2L)\mu C_i(V_g - V_0)^2 \qquad (1)$$

where I_{ds} is the drain-source current in the saturation region, W (1.5 mm) and L (1 mm) are the channel width and length respectively, μ is the field effect mobility, C_i is the capacitance per unit area of the insulating layer, and V_g and V_0 are the gate and threshold voltages. The field-effect mobilities of all rubbed films are summarized in Table 2. Compared to nonrubbed control samples deposited directly onto the substrates without the alignment layer, the oriented films have comparable and sometimes enhanced mobilities along the rubbing direction. The reasons for the differences in mobility among the various materials are associated with the film morphology and will be discussed later in the morphological section. The mobilities perpendicular to the rubbing direction are lower by more than 15 times than along the rubbing direction.

It has been shown previously that the active charge conduction region for an organic field-effect transistor is located at the organic/dielectric interface.[2,12] The anisotropic mobility ratios were found to be much higher than the dichroic ratios obtained from the absorption spectra, suggesting possibly better molecular alignment at the organic/dielectric interface than in the bulk film overall. This is very reasonable in view of the better alignment attained close to the template surface. In addition, the linear grooves along the rubbing direction (as already suggested by the AFM images) may have a significant impact on the electrical characteristics (see also the next section). We should also note that the channel length (L) for our transistors is relatively large (order of millimeters). The fact that high anisotropy ratios can be obtained uniformly over the entire film with such large feature sizes is a clear indication of good macroscopic alignment in our films. Better anisotropy ratios and possibly higher mobilities may be obtained with smaller feature sizes by reducing roughness, groove formation, and grain boundaries.

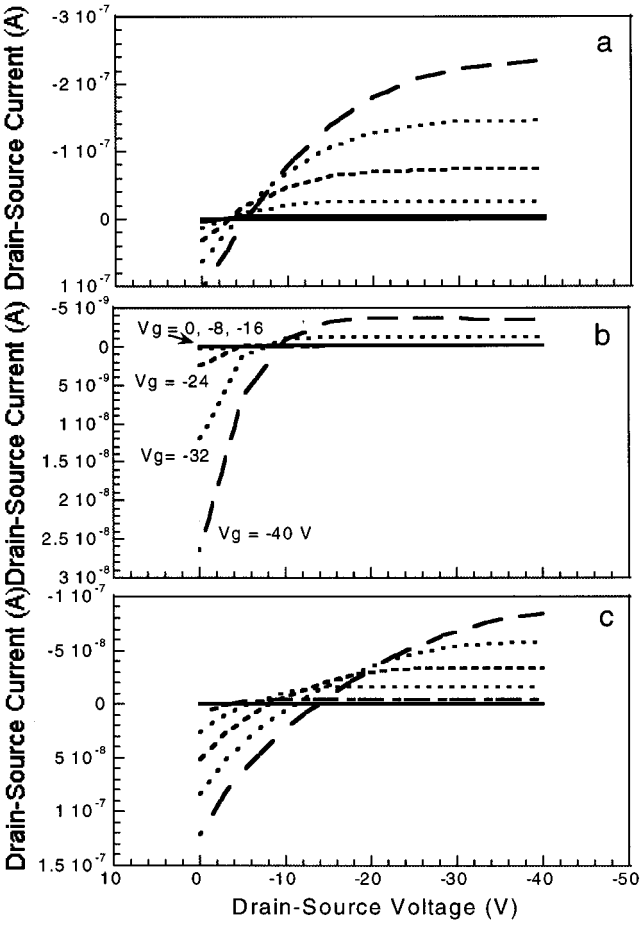

Figure 4. Drain-source current vs drain-source voltage for a CuPc film oriented (a) parallel and (b) perpendicular to the rubbing direction. (c) Drain-source current vs drain-source voltage for a nonrubbed CuPc film. Gate voltages are −8, −16, −24, −32, and −40 V from lower to upper curves.

An interesting feature is seen when comparing the leakage currents through the dielectric layer (as functions of increasing gate voltage), shown as the increasing deviation from zero current at zero drain-source voltage in Figure 4. These leakage currents are generally caused by leakage through the dielectric layer as a result of pinholes or defects mediated by conduction through nonpatterned semiconductor. They can be reduced by patterning the gate electrodes and/or the semiconducting layer. We found that these leakage currents were noticeably lower in rubbed films (Figure 4a,b) without the need for patterning the semiconducting layer and the gate electrodes. These results suggest that aligned films can eliminate conduction pathways along certain directions and reduce cross-talk between transistors, thus offering similar effects as patterning the semiconducting layer.

III. Morphological Studies. The morphology of α-6T sublimed onto rubbed α-6T is seen in the bright-field transmission electron micrograph of Figure 5a; the rubbing direction is identified by a double arrow. It is clear from these micrographs that the sublimed α-6T molecules form edge-on crystals 20−40 nm thick that are inclined to the rubbing direction. The crystals are in (crystallographically) twinned orientation to each

(39) Wittmann, J. C.; Straupe, C.; Meyer, S.; Lotz, B.; Lang, P.; Horowitz, G.; Garnier, F. *Thin Solid Films* **1998**, *333*, 272−277.

Table 2. Field Effect Mobilities of Rubbed Organic Small Molecules and Anisotropic Ratios of Mobilities in Different Directions[a]

	parallel to rubbing direction	perpendicular to rubbing direction	mobility anisotropy ratio	nonrubbed control samples
α-6T	0.0075−0.0085	no activity−0.00016	>50:1	0.01
α-6P	0.0045−0.0055	no activity−0.00016	>550	0.02
pentacene	0.24−0.25	no activity−0.0006	>40:1	0.15
CuPC	0.0018−0.0022	no activity−0.00013	>15:1	0.001
FCuPc	0.021−0.023	no activity−0.00008	>40:1	0.019

[a]Channel width of 1.5 mm and length of 1 mm are used for TFT fabrication. Also shown for comparison are the mobilities obtained from non-rubbed samples.

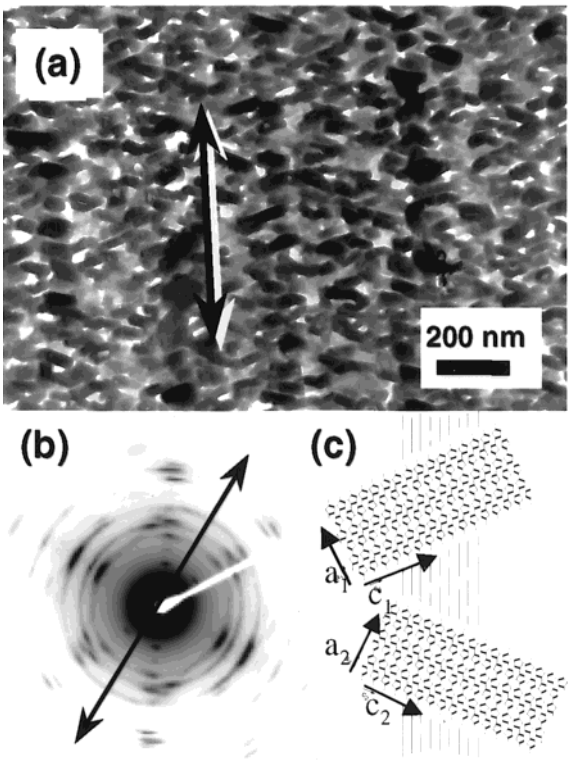

Figure 5. (a) Transmission electron micrograph of α-6T evaporated onto an aligned α-6T film. (b) The corresponding selected-area diffraction pattern with the electron beam perpendicular to the substrate. (c) Schematic of molecular and unit-cell orientations of α-6T evaporated onto rubbed α-6T, yielding the observed pseudo-twinned arrangement of the sublimed crystals.

other with their composition plane parallel to the rubbing direction (i.e., to the axis of the underlying molecules). The lamellar normals form an angle of ca. 47° in agreement with the angle between the two major rows of reflections seen in the corresponding selected-area diffraction pattern in Figure 5b. These rows correspond to two twinned *h*00 series, with observed reflections extending beyond 24 0 0. These results therefore indicate that the crystallographic arrangements between evaporated and rubbed molecules of α-6T are as shown schematically in Figure 5c. Thus, the two populations of sublimed crystals are not in actuality physically twinned to each other but only a result of nucleation in one of two populations symmetrically disposed to the substrate α-6T molecules in the manner seen in Figure 6c.

We should note that essentially the same growth pattern of crystals was observed by Wittmann et al. for α-6T that had been evaporated onto a highly oriented

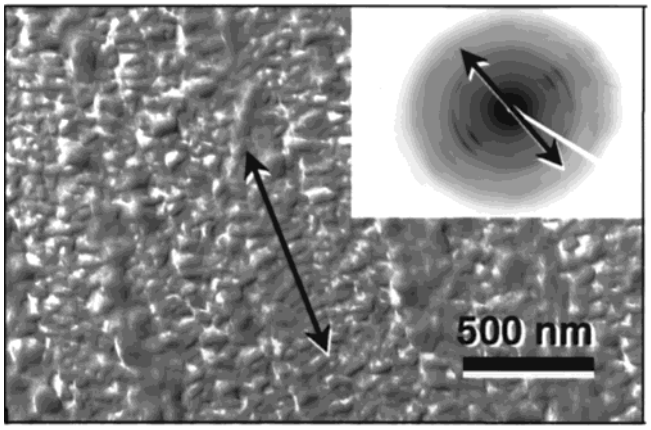

Figure 6. Transmission electron micrograph obtained after evaporation of α-6T onto an aligned α-6T film (by soft-hair brush). Inset, corresponding selected-area diffraction pattern with the electron beam perpendicular to the substrate.

PTFE friction-transferred surface.[39] The composite electron-diffraction patterns obtained were analyzed in great detail in this important publication and will therefore not be discussed further here. However, in our case, no reflections due to oriented PTFE are visible, consistent with our AFM discussion (Figure 3) of no observable traces of PTFE on the rubbed surface.

To further confirm that the observed edge-on crystal growth of α-6T sublimed onto rubbed α-6T is not the result of traces of aligned PTFE molecules left behind during our ambient-temperature rubbing, we performed the same experiment using instead a soft-hair brush. With it, we gently brushed an α-6T film (5 nm thick) before subliming onto it a thick (50 nm) layer. The corresponding morphology and electron-diffraction patterns are seen in Figure 6. The diffraction pattern is similar to that in Figure 5 but, of course, shows much poorer orientation (as is expected from the use of a soft-hair brush). The morphological features in Figure 6 confirm the existence of molecular alignment and edge-on crystal deposition as obtained with PTFE. However, they clearly show that the overall orientation is far less perfect. Many crystals are seen tilted or even flat-on with respect to the substrate rather than edge-on as obtained with PTFE rubbing (Figure 5). In addition, the pseudo-twinning is also less extensive and regular.

Returning to Figure 5, we can now understand the influence of these morphological features on the macroscopic mobility of the samples. Hopping between the crystals greatly reduces mobilities,[41] so that the overall

(40) Lovinger, A. J.; Davis, D. D.; Dodabalapur, A.; Katz, H. E.; Torsi, L. *Macromolecules* **1996**, *29*, 4952−4957.

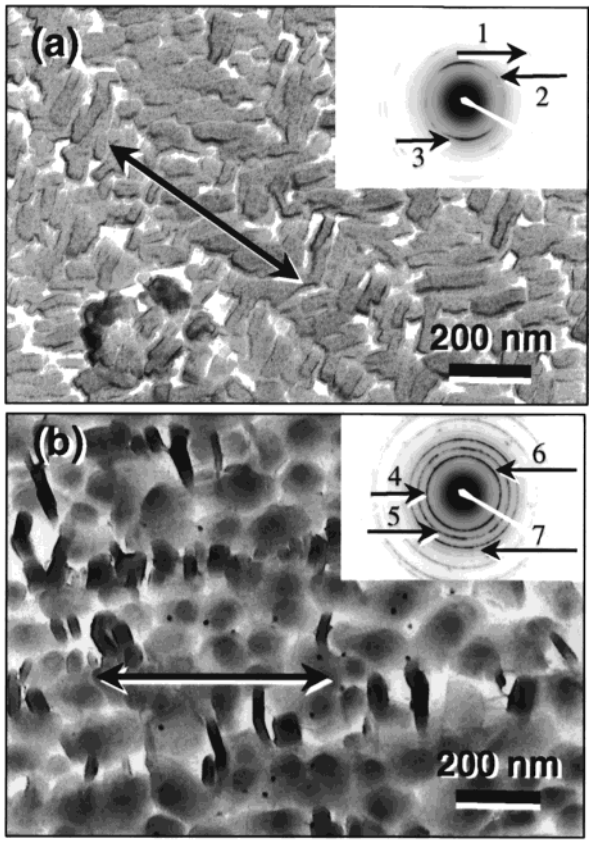

Figure 7. Transmission electron micrographs of (a) α-6P evaporated onto an aligned α-6P film and (b) pentacene evaporated onto an aligned pentacene film. Inset: corresponding selected-area diffraction pattern with the electron beam perpendicular to the substrate. Key: 1, 0.215 nm, 12th order; 2, 0.43 nm, 6th order; 3, 0.444 nm; 4, 0.45 nm; 5, 0.37 nm; 6, 0.71 nm; 7, 0.31 nm.

mobility in the rubbing direction is similar to that of ordinary (nonrubbed) sublimed α-6T films.[42] On the other hand, in the transverse direction the crystals are significantly separated from each other, not only because of the double orientation, but also because the rubbing procedure invariably introduces channels (gaps) between the molecules. As a result, the mobility perpendicular to the rubbing direction is 50 to 100 times lower than parallel to it, which is similar to the anisotropy measured for single crystals.[41] If the crystal growth can be controlled so that the crystallites grow in intimate contact, increased mobility is expected. Indeed, we saw improved mobility for copper phthalocyanine and perfluorinated copper phthalocyanine films prepared in the same way, as discussed later in this article.

Moving now on to the other rigid-rod material in our study, i.e., to α-6P evaporated onto rubbed α-6P, we find that its morphology is very similar to that of the corresponding α-6T films. Using the unit-cell parameters of Althouel et al.,[43] the row of multiple-order reflections in the electron diffraction pattern shown in Figure 8 is identified as the 00*l*. The prominent 006 spot

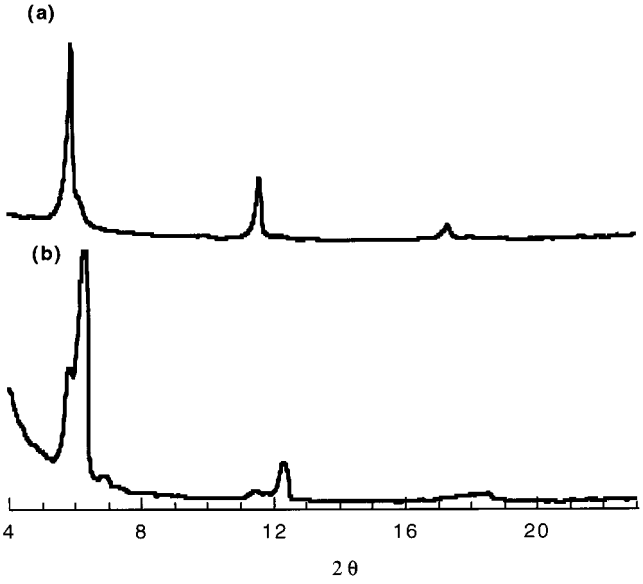

Figure 8. X-ray diffractograms obtained after evaporation of pentacene onto an aligned pentacene film: (a) deposited at room temperature; (b) deposited at 80 °C.

corresponding to the monomeric repeat is seen at 0.430 nm. X-ray diffractograms of our films also show a series of 00*l* peaks corresponding to the common polymorph of α-6P but also include a small shoulder on the low-angle side indicative of the recently found phase II. [43] Yoshida et al.[44,45] recently reported that α-6P crystallized onto uniaxially oriented poly(*p*-phenylene) has its molecules and the (203) planes parallel to the substrate. For deposition onto alkali halide substrates, a different orientation was observed.[45] The (203) orientation is also the more likely one in our case.

The morphology of α-6P deposited onto uniaxially rubbed α-6P is seen at two different magnifications in the transmission electron micrograph of Figure 7a. As in the case of α-6T, two populations of edge-on crystals are observed symmetrically inclined about the rubbing direction. The molecular axis is inclined to the *c*-axis of the unit cell by ca. 26°, and indeed the angle between the lamellar normals is 50−52°. As is seen clearly in these micrographs, the crystals are quite thick (50−100 nm) and even though they are in a crystallographically twinned arrangement, hardly any appear to be true morphological twins (i.e., growing from a joint composition phase).

These micrographs also shed some light in regard to the high anisotropy in the measured mobilities. The mobility along the rubbing direction benefits from the charge delocalization along the molecular axis in single crystals but is severely reduced by the observed poor contacts among crystals. On the other hand, the mobility in the perpendicular direction is expected to be negligibly small because of the long channels and grooves separating these crystals; these are a byproduct of the rubbing procedure and are clearly visible in Figure 7a.

The morphology and crystallography of pentacene deposited onto uniaxially rubbed pentacene are seen in

(41) Schon, J. H.; Kloc, C.; Laudise, R. A.; Batlogg, B. *Appl. Phys. Lett.* **1998**, *73*, 3574−3576.
(42) Horowitz, G.; Hajlaoui, M. E. *Adv. Mater.* **2000**, *12*, 1046−1050.
(43) Athouel, L.; Froyer, G.; Riou, M. T.; Schott, M. *Thin Solid Films* **1996**, *274*, 35−45.
(44) Yoshida, Y.; Takiguchi, H.; Hanada, T.; Tanigaki, N.; Han, E. M.; Yase, K. *Appl. Surf. Sci.* **1998**, *132*, 651−657.
(45) Yoshida, Y.; Takiguchi, H.; Hanada, T.; Tanigaki, N.; Han, E. M.; Yase, K. *J. Cryst. Growth* **1999**, *199*, 923−928.

the electron micrograph and corresponding diffraction pattern of Figure 7b. In contrast to α-6T and α-6P, pentacene does not exhibit a predominantly edge-on orientation of its crystals. The underlying molecular alignment of the rubbed substrate layer is clearly evident in Figure 7b (left-to-right). However, only a very small fraction of the crystals are seen to be edge-on; this is also confirmed by the lack of high orientation in the corresponding electron-diffraction pattern (Figure 7b inset). It is also consistent with the X-ray diffractogram of thin films of pentacene deposited at room temperature as above (Figure 8). This diffractogram shows a series of peaks arising from molecules essentially perpendicular to the substrate and corresponding to the "thin-film orientation" [46,47] with a primary peak at 1.55 nm. However, as seen from the shoulder on the high-angle side of the peak, a small amount of the "bulk phase" with the 1.45 nm repeat is also obtained. On the other hand, for pentacene deposited at 80 °C onto rubbed pentacene (Figure 8b) the intensity ratio is now reversed, showing a predominance of the "bulk phase". [46]

From all of the above, we expect that the mobility along the rubbing direction should in general be commensurate to that of ordinary sublimed pentacene, with some improvement from the uniaxially aligned molecules (as our electrical measurements in fact confirm). On the other hand, the transverse direction is once again going to be susceptible to interruption in the pathways of the charges as a result of the occasional gaps created by the rubbing step. This may explain the high anisotropy observed in uniaxially rubbed pentacene.

The findings from CuPc and FCuPc are mutually very similar. X-ray diffractograms from the former after room-temperature deposition onto rubbed CuPc show the strong 1.29 nm peak described previously,[14] which arises from the interlayer spacing of stacks of tilted molecules.[14] When CuPc is deposited at −80 °C, the diffractogram shows extremely poor crystallinity (a very weak and wide peak in the 7° 2θ region) and indeed very low mobility (in the 10^{-4} range, with a slight 2.5:1 anisotropy ratio). This is primarily attributable to the ultrathin rubbed substrate layer, since we have previously shown that the evaporated film on its own has a mobility about 1 order of magnitude lower.[14]

The morphology of room-temperature CuPc films sublimed onto rubbed CuPc is seen in Figure 9a. The crystallites have extremely small lateral dimensions (ca. 30−80 nm) and no regular crystallographic faceting. No orientation is detectable within the individual crystals. Nevertheless, they are in fact nucleated in a reasonably aligned manner dictated by the underlying molecules: one can clearly discern such rows of CuPc grains parallel to the rubbing direction (arrow in Figure 9a). The accompanying electron-diffraction pattern (Figure 9a inset) also shows a small degree of preferred orientation. These results then help explain the slight improvement in mobility over the unoriented samples, as well as the substantial anisotropy ratio between longitudinal and transverse directions.

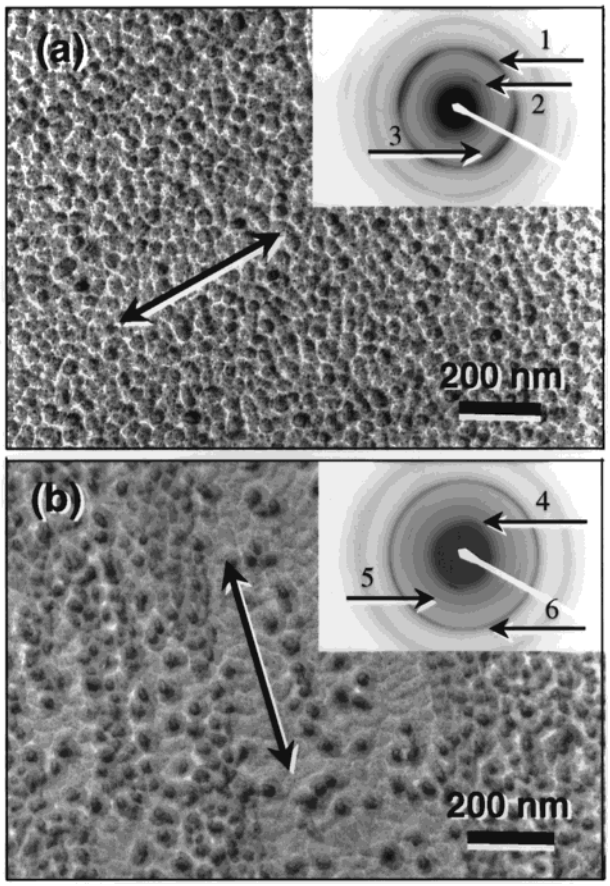

Figure 9. Transmission electron micrograph of (a) CuPc evaporated onto an aligned CuPc film and (b) FCuPc evaporated onto an aligned FCuPc film. Inset: corresponding selected-area diffraction pattern with the electron beam perpendicular to the substrate. Key: 1, 0.32 nm; 2, 0.60 nm; 3, 0.35 nm; 4, 0.69 nm; 5, 0.48 nm; 6, 0.31 nm.

For FCuPc, the same trends are observed. Its X-ray diffractogram is dominated by a peak at 1.45 nm, reflecting a similar structure and orientation as CuPc but in a lattice slightly expanded by the presence of the fluorine atoms (see Figure 2 of ref 8). Our morphological findings (Figure 9b) reveal the same type of very small, irregular crystallites as in CuPc. Here, however, the alignment imparted by the rubbed substrate appears to be more effective, as seen by the distinct rows of grains in the rubbing direction (arrow). This more effective alignment is also likely responsible for the higher anisotropy ratio obtained in this material (40:1). As for α-6T and α-6P, rubbing may be introducing microscopic grooves to the FCuPc substrate (reflected in the very distinct thickness variations across Figure 9b), which would contribute to the reduction in mobility across the transverse direction.

Conclusions

Macroscopically oriented organic semiconducting films were prepared by vacuum deposition onto rubbed substrates of the same compounds. Polarized absorption spectra and X-ray diffractograms demonstrated that the long axes of the conjugated molecules were highly oriented along the rubbing direction and parallel to the substrates. Field-effect transistors were successfully

(46) Bouchoms, I. P. M.; Schoonveld, W. A.; Vrijmoeth, J.; Klapwijk, T. M. *Synth. Met.* **1999**, *104*, 175−178.
(47) Gundlach, D. J.; Jackson, T. N.; Schlom, D. G.; Nelson, S. F. *Appl. Phys. Lett.* **1999**, *74*, 3302−3304.

fabricated using these oriented films. The resulting mobilities were anisotropic with ratios in the range of 15−100. The corresponding thin-film morphologies were examined by electron diffraction and transmission electron microscopy, which allowed us to correlate and explain the anisotropy in mobilities. The growth method studied here was shown to be applicable to several common organic semiconducting materials and seems to be an efficient general method for achieving macroscopic orientation and anisotropic electrical characteristics in the film plane.

Acknowledgment. We thank Dr. Howard Katz for providing the α-6T for this study.

CM0008563